Integrated cooling for optoelectronic devices

Christopher LaBounty[*a], Ali Shakouri[b], Patrick Abraham[a], John E. Bowers[a]

[a]Dept. of Electrical and Computer Engineering, Univ. of California/Santa Barbara

[b]Jack Baskin School of Engineering, Univ. of California/Santa Cruz

ABSTRACT

Active refrigeration of optoelectronic components through the use of thin film solid state coolers based on III-V materials is proposed and investigated. Enhanced cooling power comparing to the thermoelectric effect of the bulk material is achieved through thermionic emission of hot electrons over a heterostructure barrier layer. It is shown that these heterostructures can be monolithically integrated with other devices made from similar materials. Experimental analysis of an InP p-i-n diode monolithically integrated with a heterostructure thermionic cooler is performed. Cooling performance is investigated for various device sizes and ambient temperatures. Several important non-ideal effects are determined such as contact resistance, heat generation in the wire bonds, and the finite thermal resistance of the substrate. These non-ideal effects are studied both experimentally and analytically, and the limitations induced on performance are considered. The experimental results are then used to predict the improved performance of better designed coolers. These micro-refrigerators can provide control over threshold current, power output, wavelength, and maximum operating temperature in diode lasers. Heterostructure integrated thermionic (HIT) cooling is demonstrated to provide cooling power densities of several 100's W/cm^2.

Keywords: refrigeration, integrated, thermionic, cooling

1. INTRODUCTION

Optoelectronic devices such as laser sources, switching/routing elements, and detectors require careful control over operating temperature. This is especially true in current high speed and wavelength division multiplexed (WDM) optical communication networks. Long haul optical transmission systems operating around 1.55 μm typically use erbium doped fiber amplifiers (EDFA's), and are restricted in the wavelengths they can use due to the finite bandwidth of these amplifiers. As more channels are packed into this wavelength window, the spacing between adjacent channels becomes smaller and wavelength drift becomes very important. Temperature variations are the primary cause in wavelength drift, and also affect the threshold current and output power in laser sources. Distributed feedback (DFB) lasers and vertical cavity surface emitting lasers (VCSEL's) can generate large heat power densities on the order of kW/cm^2 over areas as small as 100 μm^2 [1]. Typical temperature-dependent wavelength shifts for laser sources are on the order of 0.1 nm/°C. Therefore a temperature change of only a few degrees in a WDM system with a channel spacing of 0.4 nm would be enough to switch data from one channel to the adjacent one, and even less of a temperature change could dramatically increase the crosstalk between two channels. Temperature stabilization is commonly performed with conventional thermoelectric coolers (TE), however since integration with optoelectronic devices is difficult [2], component cost is greatly increased because of packaging. The reliability and lifetime of packaged modules is also usually limited by that of the TE cooler [3].

An alternative solution to thermal management needs is to incorporate heterostructure integrated thermionic (HIT) refrigerators with optoelectronic devices [4,5]. These thin film coolers use the selective thermionic emission of hot electrons over a heterostructure barrier layer. This evaporative cooling occurs since the hot electrons that are on one side of the Fermi energy are emitted. In order to maintain the quasi equilibrium Fermi distribution, lower energy electrons absorb thermal energy from the lattice at the junction. The emitted electrons then redeposit their energy after passing over the barrier. Since these thin film coolers can be made with similar III−V semiconductor materials, monolithic integration with optoelectronics

* Email: labounty@engineering.ucsb.edu

Report Documentation Page

Form Approved
OMB No. 0704-0188

Public reporting burden for the collection of information is estimated to average 1 hour per response, including the time for reviewing instructions, searching existing data sources, gathering and maintaining the data needed, and completing and reviewing the collection of information. Send comments regarding this burden estimate or any other aspect of this collection of information, including suggestions for reducing this burden, to Washington Headquarters Services, Directorate for Information Operations and Reports, 1215 Jefferson Davis Highway, Suite 1204, Arlington VA 22202-4302. Respondents should be aware that notwithstanding any other provision of law, no person shall be subject to a penalty for failing to comply with a collection of information if it does not display a currently valid OMB control number.

1. REPORT DATE	2. REPORT TYPE	3. DATES COVERED
2000		**00-00-2000 to 00-00-2000**

4. TITLE AND SUBTITLE
Integrated cooling for optoelectronic devices

5a. CONTRACT NUMBER
5b. GRANT NUMBER
5c. PROGRAM ELEMENT NUMBER

6. AUTHOR(S)

5d. PROJECT NUMBER
5e. TASK NUMBER
5f. WORK UNIT NUMBER

7. PERFORMING ORGANIZATION NAME(S) AND ADDRESS(ES)
Department of Electrical and Computer Engineering,University of California,Santa Barbara,CA,93106

8. PERFORMING ORGANIZATION REPORT NUMBER

9. SPONSORING/MONITORING AGENCY NAME(S) AND ADDRESS(ES)

10. SPONSOR/MONITOR'S ACRONYM(S)

11. SPONSOR/MONITOR'S REPORT NUMBER(S)

12. DISTRIBUTION/AVAILABILITY STATEMENT
Approved for public release; distribution unlimited

13. SUPPLEMENTARY NOTES

14. ABSTRACT

15. SUBJECT TERMS

16. SECURITY CLASSIFICATION OF:			17. LIMITATION OF ABSTRACT	18. NUMBER OF PAGES	19a. NAME OF RESPONSIBLE PERSON
a. REPORT	b. ABSTRACT	c. THIS PAGE			
unclassified	**unclassified**	**unclassified**		**7**	

Standard Form 298 (Rev. 8-98)
Prescribed by ANSI Std Z39-18

is possible. The result of this integration is an extended component lifetime and a very fast cooling response due to the small thermal mass of the cooler. Furthermore, standard integrated circuit batch fabrication techniques can be used to manufacture these coolers, where as TE coolers use a bulk fabrication process. Another advantage of a HIT cooler is the dramatic gain in cooling power density.

To demonstrate monolithic integration of a device with a HIT cooler, a simple InP p-i-n diode was grown on top of a 1 µm thick InGaAs/InGaAsP HIT cooler. Cooling performance was investigated for various current biases through the diode which corresponds to effectively changing the thermal load. After discussing the measurements, the non-ideal parasitic effects are identified and examined. These results are then used to predict the effectiveness of HIT coolers integrated with diode lasers.

2. DEVICE STRUCTURE

The HIT cooler structure consisted of a 1 µm thick superlattice barrier (25 periods of 10 nm InGaAs and 30 nm InGaAsP, λ=1.3 µm) surrounded by n+ InGaAs cathode and anode layers grown by metal organic chemical vapor deposition (MOCVD). The cathode and anode layers were 0.3 µm and 0.5 µm thick respectively. On top of these layers, a 0.85 µm thick p-i-n diode was grown during the same MOCVD growth. In two wet etching steps, two stacked mesas are defined corresponding to the diode on top of the cooler as shown in figure 1. The cooler mesa's ranged in size from 20x40 μm^2 to 100x200 μm^2, and the diode size was one half that of the cooler size. Ti/Pt/Au was used to make ohmic contacts to both the p- and n-type material. The substrate was thinned to approximately 125 µm before the backside metal was deposited. The integrated devices were then cleaved, packaged, and wire bonded for testing.

3. MEASUREMENT

The diode serves two purposes in the measurement. By changing the current through the diode we can effectively change the heat load of the cooler, and by also monitoring the voltage across the diode, we can measure the temperature [6] on the cold side of the cooler, T_C. The temperature sensitivity near room temperature was determined to be 1.936 mV/°C at a bias of 1 mA. The measurement set-up is illustrated in figure 2. A constant current (I_D) was sent through the diode and the diode voltage (V_D) was monitored as the cooler current (I_C) was varied. The resistors of figure 2 represent the parasitic wire bonds that add to the heat load on the device. The measured voltage can be expressed as

$$V_M = (R_{D1} + R_{D2}) I_D + V_D + \frac{\boldsymbol{r}_c}{A_c}(I_D + I_C) \tag{1}$$

where R_{D1} and R_{D2} are the wire bond resistances, $\boldsymbol{r}_c$ is the contact resistivity, and A_c is the area of the metal contact on the cooler. If equation 1 is rearranged to solve for V_D as a function of I_C, then the resulting expression is equal to the measured voltage minus some constant values and minus a value that changes with respect to I_C, that is $\boldsymbol{r}_c\, I_C / A_C$. Therefore to correctly measure the temperature on top of the device, the contact resistivity must be determined. Once V_D is known, the temperature can be calculated using the conversion values for the corresponding diode current as given above for 1 mA.

The thermionic heating and cooling are proportional to current and can be expressed as (in the limit of Boltzmann statistics)

$$Q_{TI} = (\boldsymbol{f}_B + \frac{2k_B T}{e}) \cdot I \tag{2}$$

where $\boldsymbol{f}_B$ is the heterojunction barrier height, k_B is Boltzmann's constant, and e is the charge of an electron [5]. Since cooling is linearly proportional to current and Joule heating is proportional to the square of current, temperature versus current is determined by a second order polynomial. This can best be described by the expression for overall cooling power

$$Q_l = Q_{TI} - \frac{\boldsymbol{r} d}{A_c} I_C{}^2 - \frac{\boldsymbol{b}}{d} \Delta T \tag{3}$$

where $\boldsymbol{r}$ is the electrical resistivity of the cooler, d is the thickness of the cooler, $\boldsymbol{b}$ is the thermal conductivity between hot and cold junctions, and $\boldsymbol{DT}$ is the temperature difference across the cooler. When this expression is solved for $\boldsymbol{DT}$, the terms in the second order polynomial are apparent.

4. RESULTS

A direct way of measuring the temperature of the device is to use a micro-thermocouple. Device "A" from figure 3 shows the temperature versus current for the cold side of a 70x140 μm^2 cooler that had the integrated diode removed by selective wet etching. The temperature data was curve fit with a second order polynomial resulting in a linear coefficient of 3.53 °C/A, and a quadratic coefficient of 3.37 $°C/A^2$. Since this cooler structure was identical to the one with the integrated diode (device "B"), the two devices should have the same linear coefficient. The quadratic coefficient, on the other hand, may differ since it is dependent on processing variations such as contact resistance, packaging and wire bonding. Consequently the contact resistance ($\boldsymbol{r}_C$) can be determined from equation (1) by adjusting its value until the linear coefficients match. Using this method, device "B" from figure 3 also shows the temperature versus current for the cold side of a cooler with an integrated diode biased at 1 mA. The performance is much worse due to poor packaging and a higher contact resistance. For device "B" the contact resistance was determined to be $4.4\times10^{-6}\ \Omega cm^2$. The contact resistance for device "A" was measured by the transmission line model [7] and was estimated to be roughly $5\times10^{-7}\ \Omega cm^2$. Knowing the contact resistance, the current through the diode was increased, and the temperature versus cooler current was again measured. By changing the diode current, the heat load is changed. Figure 4 shows the maximum cooling on top of the device as a function of heat load. The dependence of cooling on the heat load density can be described in a similar manner to that of a thermoelectric device [8],

$$T_C = T_{C-\max} \cdot (1 - \frac{Q_l}{Q_{l-\max}}) \tag{3}$$

where T_C is the cold side temperature, Q_l is the heat load density, and T_{C-max} & Q_{l-max} are the corresponding maximum values. From figure 4 we find that the maximum cooling was 0.39 °C, and the maximum heat load density was 93 W/cm^2 considering only heat generation by the diode. In addition to the diode there is a constant heat load due to the two wire bonds attached to the diode (R_{D1} & R_{D2}), and another heat load due to the wire bond to the cooler (R_C) which changes with changing cooler current. In fact, much of the improvement from device "B" to device "A" in figure 3 can be attributed to the shorter wire bonds. The wire bond length should not be too short however, or else the heat conduction through the wire from the cold side to the heat sink will begin to become an issue. It is useful to examine the magnitudes of the various sources of heat that are contributing to the total applied thermal load. Figure 5 shows the heat load density versus the respective current bias for the dominating sources of heat. For small temperature differences, it was assumed that approximately one half the heat generation in the wire bonds arrives at the device. The heat load density for the diode contact resistance and wire bonds is not shown since it was several orders of magnitude smaller due to the small value of diode current. At the optimum cooler current bias of 160 mA (device "B" from figure 3), there is an additional 47 W/cm^2 of heat load density due to the wire bond and an additional 18 W/cm^2 due to the contact resistance. Using these values, the actual maximum heat load density was 158 W/cm^2. Therefore device "A" that had a maximum cooling three times as much as device "B" should be able to accommodate heat load densities as high as 475 W/cm^2.

The smaller size coolers demonstrated the greatest cooling. Since a smaller device requires less current to achieve the same thermionic refrigeration, there is less current for parasitic Joule heating from the wire bonds and contact resistance, and the overall cooling is larger. Increasing the heat sink temperature also resulted in a further increase in cooling. One reason for the improvement is the larger thermal spread of carriers at higher heat sink temperatures that allows for more carriers to pass over the heterojunction barrier. The other reason is the reduced thermal conductivity of the barrier material cutting the amount of heat that returns to the cold junction.

5. APPLICATION TO LASER DIODES

In a laser diode operating near or above lasing threshold, most of the heat is generated in the vicinity of the active region due to non-radiative recombination and absorbed radiative recombination [9]. Since there is a finite thermal resistance between the active region and heat sink, the temperature of the active region will be greater than that of the heat sink. This thermal resistance is mostly due to the substrate underneath the laser and can be substantially large. By using the integrated cooler, active region temperature can be controlled more easily as the distance to the cooler can be as small as a few microns and the cooler mass is comparable to that of the laser. The active region in a typical diode laser can reach temperatures greater than 70 °C above the heat sink temperature. For these applications, the micro refrigerator does not need to cool the laser below the heat sink temperature, but only needs to provide high heat pumping densities. If the conventional cold side of the cooler

is actually hotter than that of the heat sink, then the third term in equation 3 has a positive sign and larger cooling power densities are possible. However, if substantial cooling below the heat sink temperature is desired, simulations with more optimized structures and packaging have predicted single stage cooling of 20-30 degrees with cooling power densities of several 1000's W/cm^2 [10].

Some of the laser parameters that can be controlled or improved with the integrated cooling are emission wavelength, output power, threshold current, and maximum operating temperature. If the active region of the laser, with a temperature-dependent wavelength shift of 0.1 nm/ °C, can be cooled to the heat sink temperature, then a tuning of 7 nm should be possible. This wavelength shift could also be used to monitor the temperature of the active region. Similarly, the output power for a typical DFB laser changes by approximately 0.4 dB/°C corresponding to 28 dB of power change. Furthermore, if the active region temperature could be kept close to that of the heat sink, then the maximum operating temperature of the laser would be equivalent to that of the heat sink. Finally with a cooled active region, the carrier leakage would be reduced along with the threshold current.

6. CONCLUSIONS

Monolithically integrated cooling with thin film solid state coolers has been demonstrated. Cooling power densities of several hundred W/cm^2 has been measured with an integrated InP p-i-n diode and 1 μm thick InGaAs/InGaAsP HIT cooler. The wire bonds and contact resistance were determined to add significantly to the heat load density and must be considered in an optimally packaged device. Cooler integration with diode lasers grown from similar materials is possible and it should be possible to control the characteristics of the laser sources by manipulating the cooler current.

ACKNOWLEDGMENTS

This work was supported by the Office of Naval Research and the Army Research Office through the DARPA/HERETIC program.

REFERENCES

1. J. Piprek, Y.A. Akulova, D.I. Babic, L.A. Coldren, J.E. Bowers, "Minimum temperature sensitivity of 1.55 μm vertical-cavity lasers at 30 nm gain offset," *Appl. Phys. Lett.*, Vol. 72, No. 15, (13 April 1998), pp. 1814-6.
2. L. Rushing , A. Shakouri, P. Abraham, J.E. Bowers, "Micro thermoelectric coolers for integrated applications," *Proceedings of the 16th International Conference on Thermoelectrics*, Dresden, Germany, August 1997, pp. 646-9.
3. T.A. Corser, "Qualification and reliability of thermoelectric coolers for use in laser modules," *41st Electronic Components and Technology Conference*, Atlanta, GA, USA, May 1991, pp. 150-6.
4. A. Shakouri, C. LaBounty, J. Piprek, P. Abraham, J.E. Bowers, "Thermionic emission cooling in single barrier heterostructures," *Appl. Phys. Lett.*, Vol. 74, No.1, (4 Jan. 1999), pp. 88-89.
5. A. Shakouri, E.Y. Lee, D.L. Smith, V. Narayanamurti, J.E. Bowers, "Thermoelectric effects in submicron heterostructure barriers," *Microscale Thermophysical Engineering*, 2:00-00, 1998.
6. J.M. Swartz, J.R. Gaines, "Wide range thermometry using gallium arsenide sensors," *Measurement & Control in Science & Industry*, Vol. 4, 1972.
7. G.K. Reeves, H.B. Harrison, "Obtaining the specific contact resistance from transmission line model measurements," *Elec. Dev. Lett.*, Vol. EDL-3, No.5, (1982), pp. 111-113.
8. D.M. Rowe, *CRC Handbook of Thermoelectrics*, CRC Press, New York, 1995.
9. N.K. Dutta, T. Cella, R.L. Brown, D.T.C. Huo, "Monolithically integrated thermoelectric controlled laser diode," *Appl. Phys. Lett.*, Vol. 47, No. 3, 1 August 1985, pp. 222-4.
10. C. LaBounty, A. Shakouri, G. Robinson, P. Abraham, J.E. Bowers, "Design of integrated thin film coolers" *Proceedings of the 18th International Conference on Thermoelectrics*, Baltimore, MD, USA, August 1999.

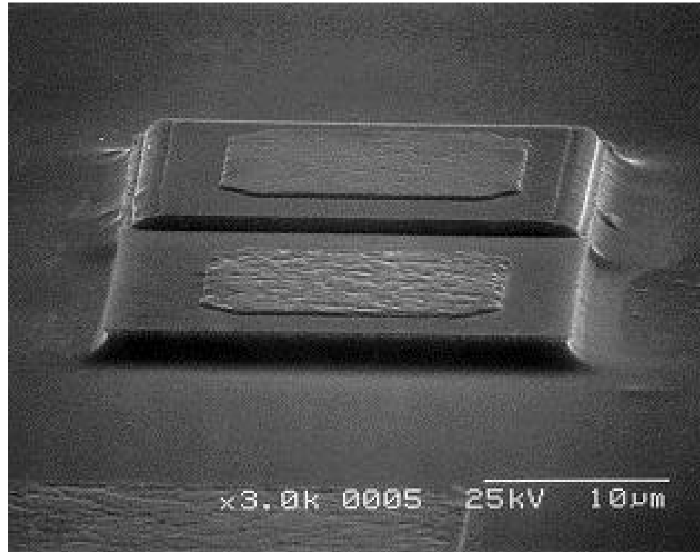

Figure 1. S.E.M. photo of a processed device showing the p-i-n diode on top of the 1 μm thick HIT cooler.

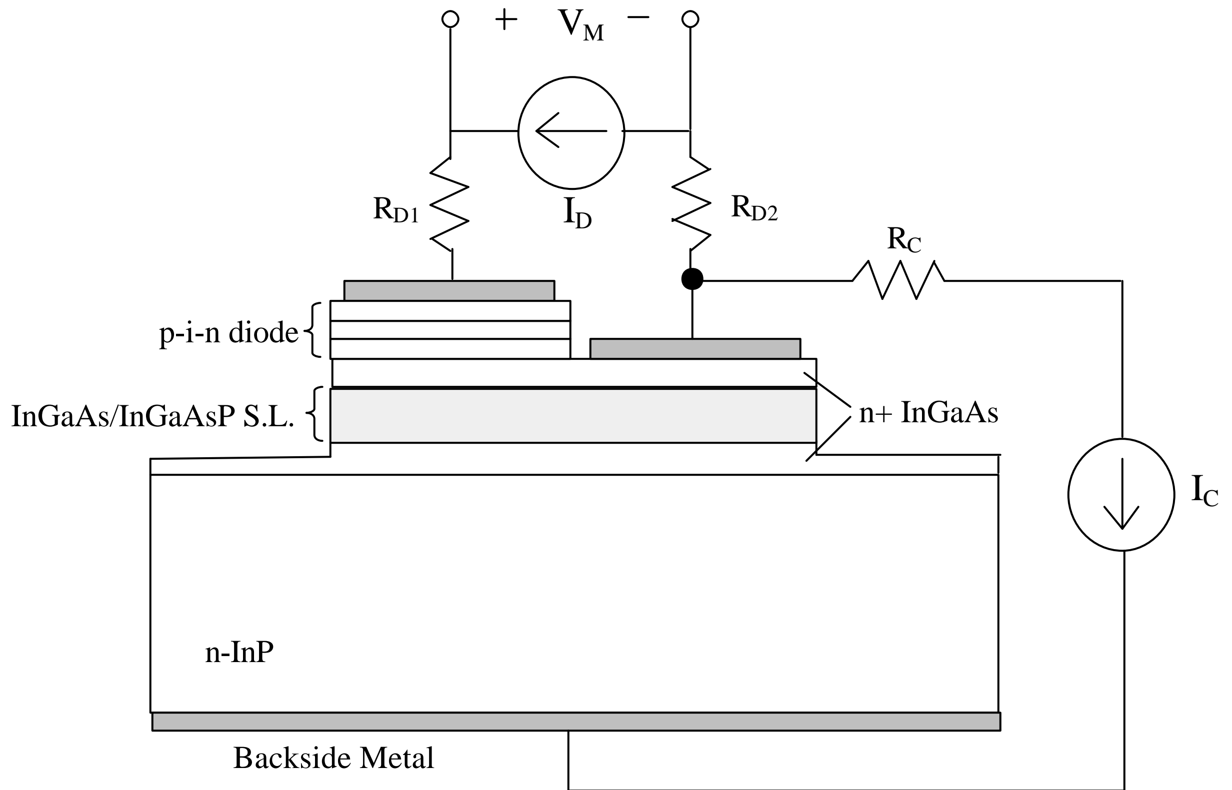

Figure 2. Set-up for measuring the temperature of the integrated diode versus the current through the cooler (I_C) and the diode (I_D). R_{D1}, R_{D2}, and R_C are the wire bond resistances.

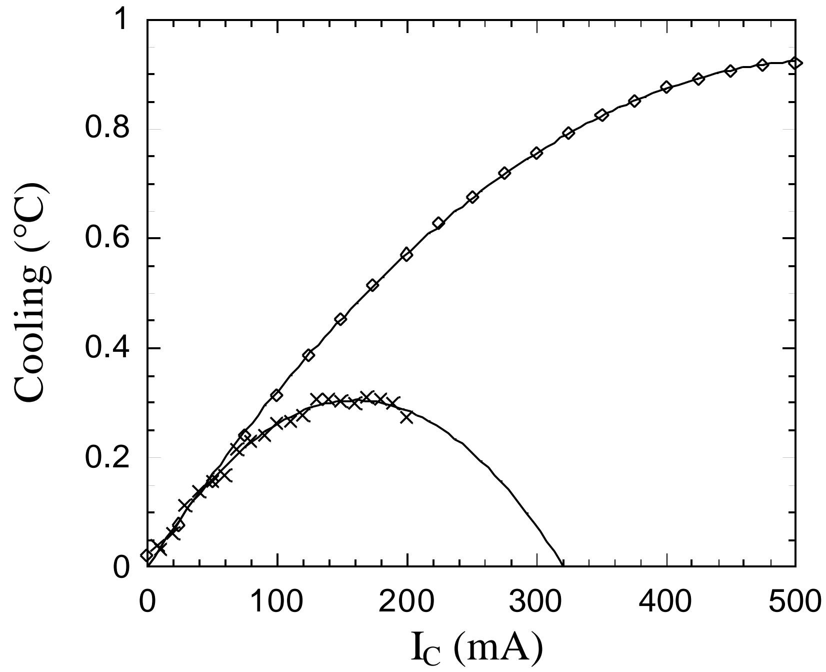

Figure 3. Measured cooling versus cooler current using a micro-thermocouple for a well packaged device (curve 1), and using the integrated p-i-n diode with poor packaging (curve 2). Both device areas were 70x140 μm^2.

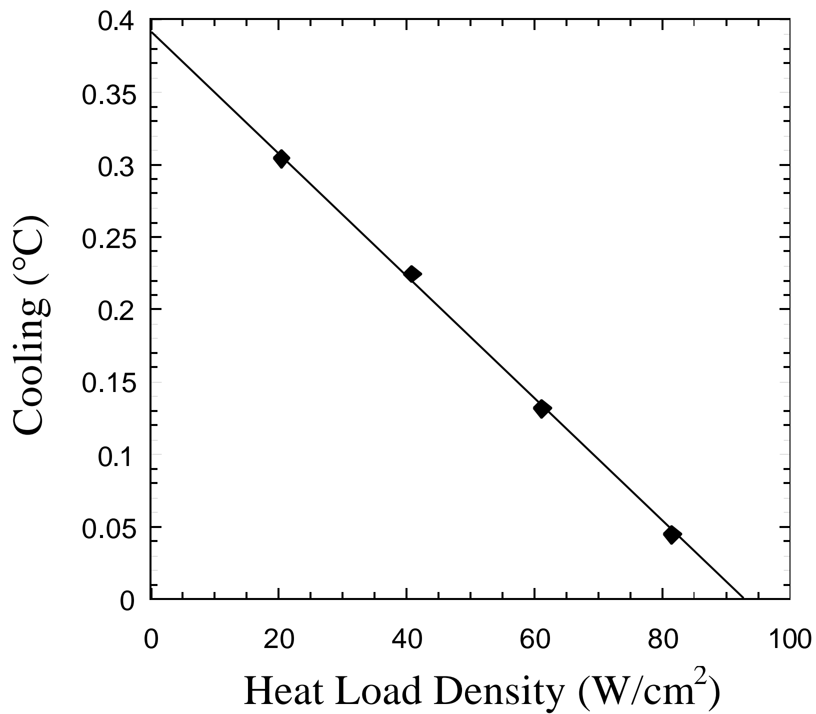

Figure 4. Cooling versus heat load density. The points are experimental data while the linear curve fit corresponds to equation (3).

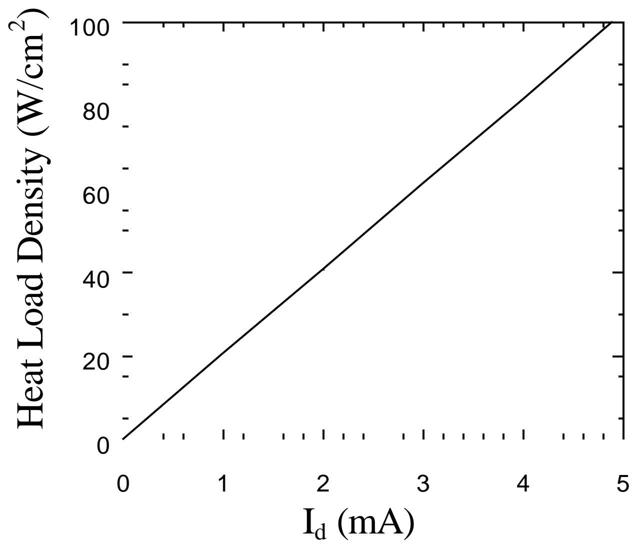

(a)

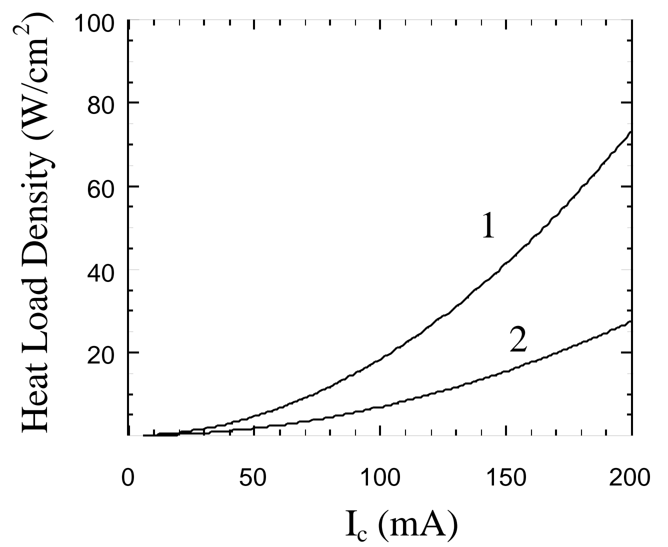

(b)

Figure 5. (a) Heat load density for the diode versus diode current. (b) Heat load density from the wire bond (curve 1) and from the contact resistance (curve 2) versus cooler current.